Journal of Molecular Structure 1006 (2011) 66–76

Contents lists available at ScienceDirect

Journal of Molecular Structure

journal homepage: www.elsevier.com/locate/molstruc

Terahertz spectroscopy: Its future role in medical diagnoses

Edward Philip John Parrott [a], Yiwen Sun [a,1], Emma Pickwell-MacPherson [b,*]

[a] Electronic Engineering Department, The Chinese University of Hong Kong, New Territories, Hong Kong
[b] Electronic & Computer Engineering, The Hong Kong University of Science & Technology, Clear Water Bay, Hong Kong

ARTICLE INFO

Article history:
Available online 13 June 2011

Keywords:
Terahertz imaging
Terahertz spectroscopy
Protein spectroscopy
Biomedical
Intermolecular interactions
Cancer

ABSTRACT

Over the past two decades, terahertz radiation has received a lot of interest due to advances in emission and detection technologies in the late 1980s and early 1990s which allowed the construction of coherent source/detection regimes. This paper focuses on reviewing the use of terahertz radiation in the investigation and understanding of biological systems and medical diagnosis. In particular, research on terahertz spectroscopy of biomolecules, from amino acids to proteins is presented, and examples of potential medical applications are discussed.

1. Introduction to terahertz radiation

The term "terahertz radiation" (1 THz = 10^{12} Hz) refers to the region of the electromagnetic spectrum that straddles both the high frequency microwave region and the long-wavelength far-infrared region. The region is commonly defined as lying between 0.1 and 10 THz. Due to the difficulties of generating radiation at these frequencies using either electronic or optical techniques, for many years this region lay relatively unexplored, giving rise to the term "terahertz gap". The importance of bridging this gap is highlighted in Fig. 1 where it can be seen that numerous molecular vibrations are present in this frequency range. Molecular rotations, low frequency bond vibrations and crystalline phonon vibrations are all present in this frequency range, and these allow a variety of phenomena to be monitored and measured, including spectral broadening in flames [1], polymorphic transformations [2], carrier dynamics in semiconductors [3,4], photoconductivity in high-mobility polymeric materials [5] and characterization of the electronic properties of carbon nanotubes [6,7]. However, perhaps of most interest within the area of medical diagnosis is the sensitivity of terahertz radiation to hydrogen bond stretches and distortions, due to their prevalence in liquid water and thus biological samples.

1.1. Generation and detection of broadband pulses of terahertz radiation

The basic operation of broadband frequency sources is based around the Auston switch, first described by Auston in 1975 as a way of gating an electrical pulse over a few picoseconds using light [8]. Until the advent of ultrafast femtosecond lasers in the late 1980s, however, it was not possible to generate short enough electrical pulses in order to produce terahertz radiation. Briefly, the Auston switch works in the following fashion. An ultrashort laser pulse is focused onto the surface of a semiconductor material (such as GaAs) whose photon energy is greater than the band-gap of the material. This promotes electrons into the conduction band, resulting in the formation of electron–hole pairs at the surface of the semiconductor. If a potential difference is applied across this surface using a pair of electrodes then the charge carriers will be accelerated across the gap, radiating away energy in the process. The key discovery by Grischkowsky and Fattinger was that this ultrafast process produced a broadband transient at terahertz frequencies that propagated through free-space [9].

Detection of this terahertz radiation can be achieved either through the use of a second photoconductive switch or by using an electro-optically active birefringent crystal such as ZnTe or GaP. A photoconductive switch measures the terahertz transient by recording the current induced between two electrodes when the terahertz radiation, gated by the optical pulse, is incident on the device. The electro-optic effect works due to the fact that the birefringence change experienced by the crystal is proportional to the incident (terahertz) electric field. This birefringence change can be measured using a portion of the laser pulse derived from the same source to that which was used to excite the emitter and produce the terahertz pulse [10]. The ability to measure both the phase and amplitude of the terahertz radiation is a key strength of this technique, as it allows the frequency-dependent complex permittivity of a sample to be calculated directly from the Fourier Transform (FT) of the time-domain signal, without the need to resort to Kramers-Kroenig analysis. In addition, the coherent,

* Corresponding author. Tel.: +852 2358 5034.
E-mail address: eeemma@ust.hk (E. Pickwell-MacPherson).
[1] Present address: Medical School, Shenzhen University, Guangdong, 518060, People's Republic of China.

0022-2860/$ - see front matter © 2011 Elsevier B.V. All rights reserved.
doi:10.1016/j.molstruc.2011.05.048

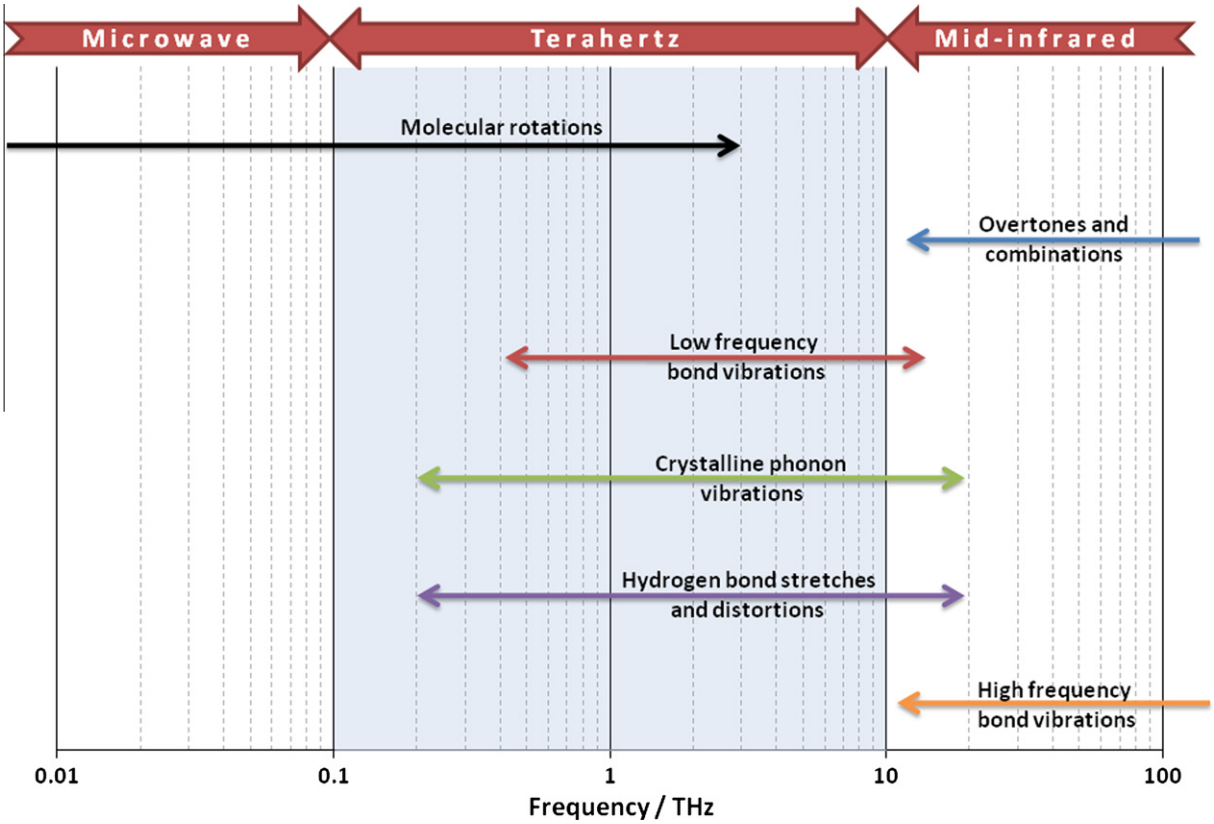

Fig. 1. Schematic illustrating the various molecular interactions in the terahertz frequency region. The terahertz "gap" is highlighted.

time-gated acquisition coupled with modulation of the terahertz beam allowing the use of lock-in techniques, gives this technique excellent noise rejection characteristics, with signal-to-noise ratios (SNR) of 10,000:1 being reported [11]. For an excellent introduction to the physics of generation and detection of terahertz radiation the reader is directed to the article by Jepsen et al. [12].

1.2. Time-domain analysis

A study of the time-domain data reveals, for the most part, information on the structural details of the sample. Fig. 2 shows

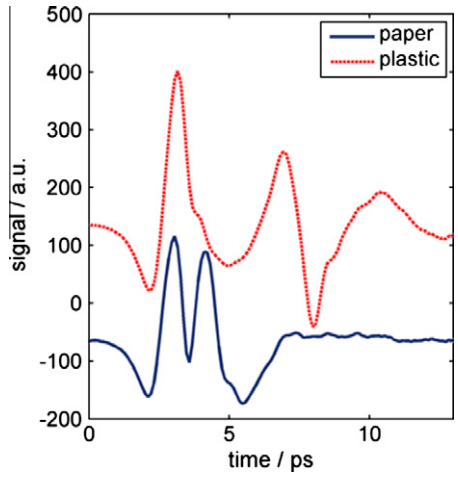

Fig. 2. Terahertz reflection time-domain pulses of a single sheet of paper (blue solid line) approximately 0.1 mm thick, and a single sheet of plastic (red dashed line) approximately 0.5 mm thick. In both cases, two distinct reflections can be determined from the time-domain traces. (For interpretation of the references to colour in this figure legend, the reader is referred to the web version of this article.)

two typical time-domain traces taken with a Teraview TPI medical probe. Both traces show two distinct peaks; these are due to the reflection of the incident terahertz pulse off two separate interfaces. The separation of these two peaks gives information on the spatial separation of the two interfaces: closer peaks imply optically thinner materials than those with peaks that are more spread out. In the example figure the paper thickness has been measured as being 0.1 mm, whereas the plastic sample is known to be 0.5 mm thick, and it can be seen that the peak separation is correspondingly different for the two samples.

However, in order to be able to estimate a real interface separation from the time-domain traces, information on the refractive index of the material is required. This can be done accurately using the frequency-domain analysis techniques outlined in the subsequent section, but the time-domain can give a useful estimation of the average refractive index (n_{sam}) which can be used to extract an approximate interface separation distance. Given the refractive index of the initial medium, n_{pre} and the incidence angle of the terahertz pulse (θ_{inc}), then Fresnel theory enables the calculation of the refractive index from the reflection coefficient (R_{ps}):

$$n_{sam} = n_{pre}\frac{\cos\theta_{Inc.}(1-R_{ps})}{\cos\theta_{tra}(1+R_{ps})} \quad (1)$$

where θ_{tra} in Eq. (1) is the transmitted radiation angle which may be calculated using Snell's law:

$$n_{sam}\sin\theta_{tra} = n_{pre}\sin\theta_{inc.} \quad (2)$$

A combination of Eqs. (1) and (2) allow the refractive index to be calculated. The reflection coefficient can be estimated from the ratio of the reflected to the incident peak-to-peak value of the terahertz transient.

1.3. Frequency-domain analysis

$$\tilde{n}(w) = n_r(w) - i\frac{\alpha(w)c}{2w}. \quad (3)$$

Fourier transform of the time-domain data retrieves the frequency dependent parameters of the pulse. In particular, it allows the extraction of the complex refractive index, from which the real refractive index and the absorption coefficient may be derived:

In Eq. (3), $\tilde{n}(w)$ is the complex refractive index, $n_r(w)$ is the real refractive index, $\alpha(w)$ is the absorption coefficient and c and w are the speed of light and the angular frequency ($w = 2\pi f$) respectively. From equation 3 it is possible to calculate the dielectric permittivity of the material, $\tilde{\epsilon}(w)$ as follows:

$$\tilde{\epsilon}(w) = \tilde{n}^2(w) = \left(n_r(w) - i\frac{\alpha(w)c}{2w}\right)^2. \quad (4)$$

Eqs. (3) and (4) give us information on the dielectric properties of the material, which in turn give an insight into other physical properties of the materials.

1.4. Introduction to intermolecular interactions

Techniques such as mid-infrared (mid-IR) spectroscopy are commonly used to identify different materials and samples. At these frequencies, commonly 500–4000 cm^{-1} (15–120 THz), the mid-IR radiation probes the high energy, high frequency intramolecular bonds such as the functional group rotations, oscillations and stretches highlighted in Fig. 3a. The frequencies of these functional group vibrational modes are well known, and the "fingerprint region" between approximately 500–1500 cm^{-1} gives a lot of information as to the chemical composition of the molecule (see Fig. 3b for an example mid-IR spectrum of malic acid).

In contrast, terahertz frequency radiation (0.1–10 THz) is lower in energy, and so the characteristic length scale of the radiation is longer than for mid-IR radiation. As a consequence, terahertz frequency radiation probes the longer-range, lower energy intermolecular modes such as the hydrogen bond torsions and librations, and whole molecule stretches, which are highlighted in Fig. 3c. It is these intermolecular modes that produce the spectral features seen in terahertz spectra of crystalline materials, such as the three distinct absorption peaks recorded by THz-TDS for malic acid shown in Fig. 3d. These intermolecular modes have been found to be sensitive to changes in the supramolecular architecture of crystalline compounds, and have been used to distinguish polymorphs [13] and cocrystals [14]. However, exploitation of this frequency range is not limited to crystalline materials, as long-range intermolecular interactions are present in almost all systems. Of particular interest to medical spectroscopy is the interaction of water and hydrogen bonds with other molecules present within biological systems, such as amino acids, peptides, DNA and proteins. The recent advances in the understanding of these molecules are outlined in the following section, before considering the macroscopic applications of terahertz spectroscopy in the medical field.

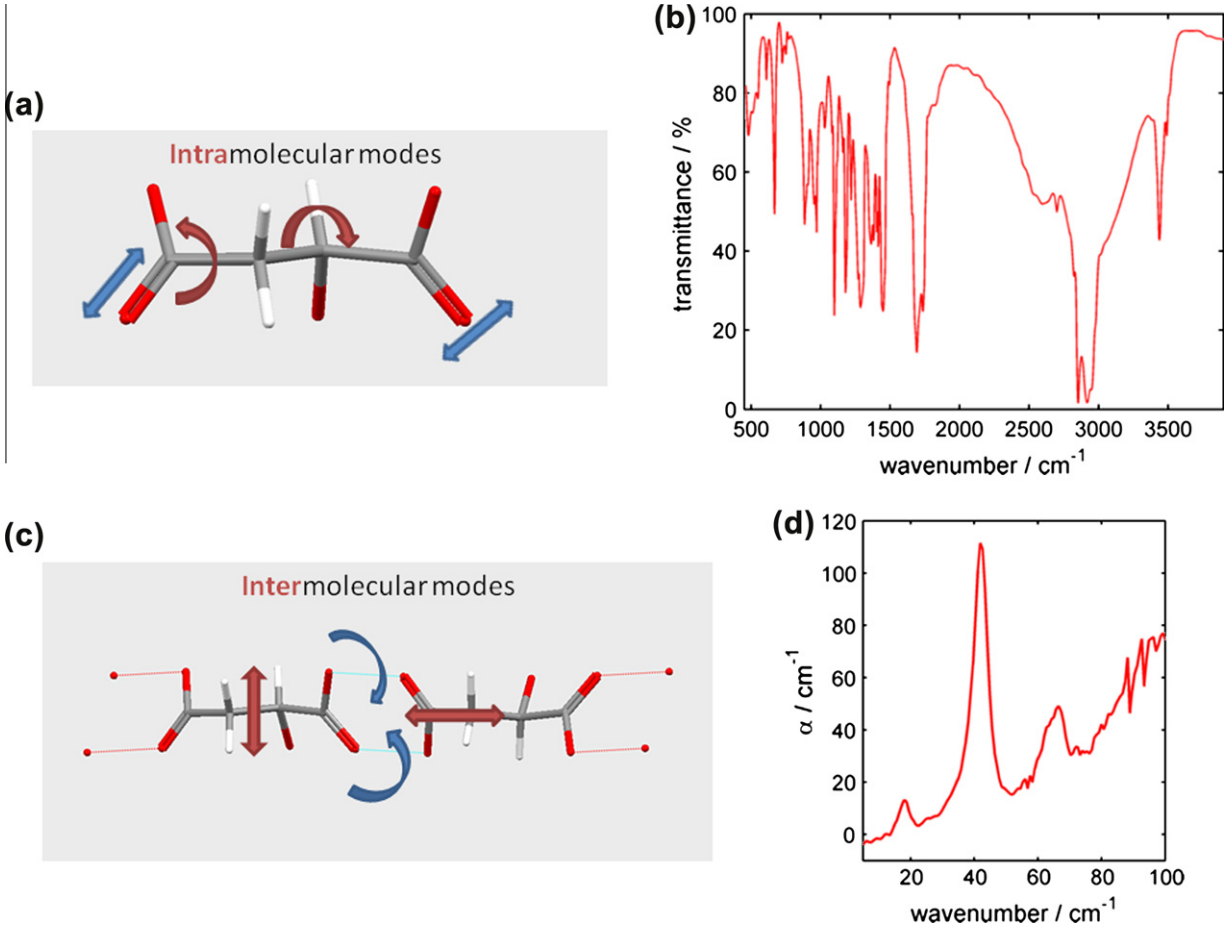

Fig. 3. DL-malic acid molecule showing representative types of (a) intramolecular and (c) intermolecular vibrational modes. The (b) mid-IR spectrum and (d) terahertz spectrum of DL-malic acid are also shown.

2. Molecular spectroscopy

2.1. Introduction

The sensitivity and specificity of terahertz spectroscopy to both biomolecular function and activity requires a detailed investigation of the biopolymer secondary and tertiary structures and their dynamic motions, including both intermolecular and intramolecular vibrations. It has been suggested that these low-frequency vibrational spectra can be used to picture the concerted vibrational modes of polypeptide chains and DNA molecules at the atomic level [15,16]. These vibrations are expected to be observed at terahertz frequencies and may be measured using Fourier Transform Infrared (FTIR), Raman and IR absorption spectroscopies. Terahertz spectroscopy has emerged as a preferred technique for accessing the low frequency regions due to its ability to simultaneously record phase and amplitude information, allowing the complex dielectric permittivity of the material to be derived (FTIR, Raman and IR measure intensity only). Of greatest interest is the ability to obtain the vibrational spectra for biological systems in the aqueous phase as this is the phase which is closest to their natural environment. However, this causes difficulties due to the strong interaction of terahertz radiation with water; as a consequence many of the protein conformational modes will be masked by the strong water absorption modes. However this may be less problematic then it may seem as researchers begin to understand the role the weak force interactions that occur during ligand binding have in the terahertz absorption characteristics.

There have been a considerable number of studies predicting the terahertz frequency vibrational spectra of biomolecules, and what is clear is that it is unlikely that such large molecules will contain sharp absorption features from specific vibrational modes. Instead, these molecules have been seen to have many overlapping states yielding essentially featureless spectra. Nonetheless, the functional differences between molecular structures, for example studies of single- and double-stranded DNA, have been seen to lead to pronounced differences in the overall terahertz dielectric properties of the material [17]. This difference has been shown to be a highly sensitive contrast mechanism for label-free detection of the hybridization state of DNA [18]. This section explores and highlights some of the key and recent findings in the area of these biomolecules, from studies of the smallest building blocks that are amino acids and peptides, to the large polypeptide proteins.

2.2. Amino acids and peptides

Amino acids are the basic building blocks of proteins. Properties such as the shape and form of each protein are dictated by the precise sequence of amino acids in it. In an effort to understand the effect of the makeup of the constituent amino acids to the terahertz spectral properties of the protein, a series of experiments were undertaken by Kutteruf and coworkers to measure the terahertz absorption features for 20 naturally occurring lyophilized amino acids [19]. The use of Fourier Transform Infra-Red (FTIR) spectroscopy enabled the authors to record an absorption spectrum for each amino acid from 33 cm^{-1} to 500 cm^{-1} (1–15 THz). These solid samples revealed numerous vibrational modes, however standard (at the time) single molecule density functional theory (DFT) calculations failed to reproduce the spectral features. This was postulated to be due to the need to include intermolecular interactions at terahertz frequencies, such as hydrogen bonding and phonon modes.

In part to understand the role of the intermolecular interactions, Korter and coworkers studied the differences in the terahertz spectra for two biomolecules [20]. The two biomolecules, 1-serine and 1-cysteine were identical except for their functional groups: –OH for 1-serine and –SH for 1-cysteine. Clear differences were observed between the two samples, especially in the low-frequency region, highlighting the effect of subtle changes in the chemical structure on the terahertz spectral features. In contrast to the earlier study, DFT calculations incorporating periodic boundary conditions were also trialed, and it was found that much better agreement with experiment was obtained using these techniques, highlighting the importance of including intermolecular interactions in the understanding of terahertz spectra.

The usefulness of using single crystals in gaining a better understanding of the 3-dimensional structure of the vibrational modes was highlighted by Rungsawang and coworkers [21]. By varying the angle of the single crystal the approximate bond directions of the various hydrogen-bonds were found for the amino acid single crystals of L-cysteine and L-histidine for the first time using angle-dependent THz-TDS, further determining the collective modes of these amino acids at terahertz frequencies.

In order to increase the range of materials and system for which THz-TDS can be applied, Kikuchi and coworkers have developed a membrane method for precipitating solid crystals out of aqueous solutions for the purpose of acquiring their spectra [22]. Terahertz spectra of the amino acids of L-threonine and Glycine were presented both as measured from the powdered forms pressed into pellets, and from crystals precipitated onto membranes that had been immersed in their aqueous solutions. This appears to be a novel method to screen some aqueous solutions for certain molecules, and could certainly be of use in testing for marker biomolecules in aqueous solutions.

Peptides are short polymers of amino acids linked by peptide bonds. They have C- and N-terminations with a specific sequence and have the same chemical structure as proteins but are shorter in length. Whilst in the far-infrared frequency range (50–500 cm^{-1}, 1.5–15 THz), investigations of solid forms have reported well-defined vibrational modes [23], it is difficult to identify the sharp spectral features for peptide mixtures with more than 10 amino acids due to the overlapping spectral density of the peptides. Yamamoto and coworkers reported the frequency-dependent absorption coefficients and the refractive indices of solid forms polyglycine and poly-L-alanine in 7–55 cm^{-1} frequency range [24]. A strong vibrational band observed at 45.5 cm^{-1} for the polyglycine was assigned to an in-plane angle bending mode of the NH···O and CO···H intermolecular bonds. Despite the prediction of a similar out-of-plane angle bend through normal mode analysis no such features were observed for poly-L-alanine, from which the authors concluded that the polyglycine has a longer-range structural order. Researchers have also begun to utilize ideas from other fields of research in order to begin to understand the observed terahertz absorption of these biomolecules. For example, Kambara and coworkers have used the universal frequency dependence of the infra-red coupling coefficient, as pioneered in the terahertz frequency studies of inorganic glasses [25–27], in order to understand the observed differences in the behavior of the β-sheet structures of various polypeptides [28].

2.3. Deoxyribonucleic acid (DNA)

As early as 1986 Wittlin and coworkers performed a range of experiments on DNA in the terahertz frequency region spanning 0.09–13.5 THz, using both microwave techniques (backward wave oscillators) and FTIR spectrometers for the low and high frequency results respectively [29]. In this study, it was found that five low-frequency vibrational modes between 40 cm^{-1} and 450 cm^{-1} gave adequate fits to the transmittance data at the three temperatures between 5 and 300 K. An absorption band at about 10 cm^{-1}, attributed to the dynamic relaxation process of the molecule, was postulated to be pronounced due to the hydration-induced absorption.

More recently, the early work of Markelz reported that the low-frequency collective modes of lyophilized calf thymus DNA were IR active at terahertz frequencies [18]. At a similar time, Brucherseifer and coworkers demonstrated the clear dependence of the complex refractive index on binding states of DNA by monitoring the time-resolved terahertz transient behavior [30]. Fischer and coworkers recorded the dielectric function of DNA nucleobases between 0.5 and 4.0 THz [31]. Numerous distinct spectral features were obtained for each nucleobase and its corresponding nucleoside. Furthermore, DFT was performed to analyse the vibrational resonances of hydrogen bonds between the molecules.

The group of Globus has undertaken a number of studies probing DNA using terahertz. Bykhovskaia and coworkers evaluated the far-IR (0–800 cm^{-1}) active modes of two DNA double-helical fragments: $(dA)_{12}\cdot(dT)_{12}$ and $(dA-dT)_6\cdot(dA-dT)_6$, which were predicted by evaluating the optical activity determined by the vibrational amplitude of the dipole moments of the molecules [32]. The calculated positions of the resonance peaks in the absorption spectrum were in good agreement with previously published FTIR spectroscopy data. In a second study of DNA, Globus and coworkers investigated the multiple dielectric resonances in the 10–50 cm^{-1} range with a high resolution of 0.2 cm^{-1} using FTIR spectroscopy [33]. The low-frequency absorption results suggested that the fine features observed in this frequency range could be used for DNA characterisation. Additional DNA studies by Globus and coworkers employed both reflection and transmission spectral measurements of the DNA samples from herring and salmon at terahertz frequencies [34]. In this work, the single stranded salmon DNA samples recorded the higher refractive index and absorption coefficients and several different vibrational modes when compared to its double stranded counterpart. This was tentatively attributed to the greater flexibility in the molecular conformation of the single stranded sample allowing for more degrees of freedom. The same group also made a comparison of the DNA spectra in both a liquid gel phase and the solid states investigated previously over the spectral range 10–25 cm^{-1} [17]. Vibrational modes are still observed in the liquid environment and are similar to those measured in the solid phase, with the width of spectral lines being approximately 0.3–0.5 cm^{-1}. Finally, some of the results for the liquid gel samples appeared to be polarisation dependent, which the authors suggested could be indicative of some sort of liquid crystal structuring.

2.4. Proteins

Much like the amino acids and peptides that constitute them, proteins interact with terahertz radiation in such a way that the protein structure and function may be elucidated. An understanding of how the vibrational modes in the terahertz region change with structure and function has been a driving factor in the research in this field. Whitmire and coworkers reported on the perceived flexibility and conformational state of Wild-Type (WT) and D96N mutant Bacteriorhodopsin using THz-TDS over a range of 2–60 cm^{-1} with a resolution of 0.17 cm^{-1} [35]. The authors found that the frequency dependence of the terahertz spectra agreed with the normal mode analysis computation; however these calculations did not predict the factor of 2 difference in the absorption values for the WT form over the mutant form. The authors attributed this result to the anharmonicity of the real potentials, which was not accounted for in their calculations. This anharmonicity appeared to be highlighted by the temperature dependence of the absorption features, with the high frequency absorption reducing at lower temperatures due to reduced population of the higher energy vibrational states. In terms of the conformational state, the terahertz results suggested that whilst the far-IR absorption of the WT protein was conformation dependent, the mutant protein displayed no conformation dependence. This result the authors interpreted as suggesting that between the two proteins measured, it was the WT protein that had the greater conformational flexibility; representing the first such study observing a conformational change through the conformational vibrational mode spectrum.

Further research carried out by Balu and coworkers in 2008 demonstrated the similarities and differences of the two photoactive protein systems – rhodopsin and bacteriorhodopsin, and improved computational modelling [36]. The authors found that the vibrational mode density at terahertz frequencies is similar in both systems, which was not unsurprising as the two proteins have a similar structure. This work suggested that large protein molecules appear to have a broad and nearly linear dielectric response, with some similarities to the mode densities, and an improved ability to correctly reproduce the calculated mode intensities. This suggested that dielectric measurements in the terahertz region should not focus solely on the glass-like response of mobile side-chains, but that the collective mode contributions of the whole molecule should also be included.

A new protein sample, hen egg white lysozyme (HEWL), was used in a series of THz-TDS measurements carried out by the group of Markelz to determine the sensitivity of terahertz to protein hydration and ligand binding [37–39]. The dielectric response of the HEWL protein was measured between 0.15 and 1.95 THz as a function of hydration [37,38]. The authors found the critical hydration transition point to be at 0.27 water/protein mass ratio. This was analysed as being the point where the first hydration shell was filled and bulk water begins to accumulate, in agreement with previous work done using NMR (Ref. [12] in [37]). The sensitivity of THz-TDS to protein–ligand binding was probed by freezing the solutions of HEWL and HEWL bound with triacetylglucosamine (3NAG) in order to remove the rotational modes of bulk water [39]. Whilst at 293 K a small decrease in α and n was observed for the HEWL + 3NAG when compared to HEWL alone, it was very similar to that of bulk water, suggesting the bulk water relaxation was the dominant term. However, at 270 K the differences between the dielectric responses for the two samples were more pronounced, and resembled more closely the results from the thin films reported previously [37]. These results suggest that the complex dielectric permittivity at terahertz frequencies can provide a unique insight into protein dynamics at critical transition points such as the relaxation response of the side chains within the protein.

We have recently investigated the effects of conjugation on an immunoglobin (IgG) protein. Absorption features were found in the peroxidase conjugated IgG (PX-IgG) shown in Fig. 4 that were not present when the same IgG was conjugated with a fluoroscein group. This emphasized very nicely how THz spectroscopy is sensitive to intermolecular interactions [40]. Additionally we have shown how, by measuring the concentration dependence of protein solutions, the hydration shell thickness around the IgG molecules can be estimated.

3. Medical spectroscopy

Due to the high attenuation experienced by terahertz radiation when propagating through aqueous environments, previous work into measuring the terahertz properties of medical tissues has been confined either to *ex vivo* samples or measurements of easily accessible surfaces, such as skin. It should be noted, however, that this large interaction that terahertz radiation exhibits in aqueous environments gives it a high sensitivity to small changes to the aqueous conditions of the materials, be it changes in the water content or changes to the chemical species present.

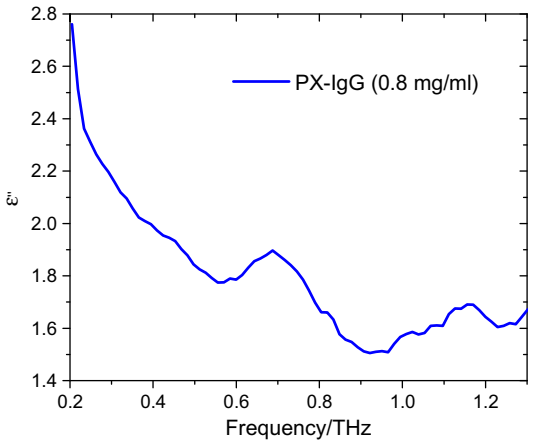

Fig. 4. Dielectric loss spectrum of peroxidise conjugated IgG (PX-IgG).

3.1. Understanding contrast

One of the first such studies of human tissues was undertaken by Fitzgerald and coworkers [41]. They measured the absorption coefficient and refractive index of a number of human tissue types, including skin, adipose tissue, striated muscle, vein and nerve, between 0.5 and 2.5 THz. Differences were observed between the different tissue types, in particular the muscle tissue displayed a higher absorption coefficient when compared to the other tissue types, suggesting a link between hydration and contrast.

In the drive to understand image contrast in medically relevant tissues, researchers have often turned to other animals from which there is a greater bioavailability, such as rats and pigs. He and coworkers measured the transmission spectra of both pork fat, lean tissue and skin, and those of lean rat tissue and rat skin [43]. Differences were observed between the different types of tissue (i.e. fat, lean and skin), with the fat tissue especially displaying a much reduced absorption coefficient when compared to the lean and skin tissues. More recently, Huang and coworkers performed a study of a number of internal rat organs, including the heart, liver, kidney and pancreas, as well as fat and leg muscle [42]. The heart sample is pictured in Fig. 5a. It was cut transversely as indicated so as to expose the internal tissue. In Fig. 5b we see that the portion of tissue to be measured has a slight hollow due to the heart chamber. When the sample is placed on the quartz window to be imaged, the hollow does not make contact with the quartz window, and the reflected signal is different and so in the terahertz image (Fig. 5c) we can locate the chamber. The region that is blue is reflected directly from the heart tissue and is used to determine refractive index, absorption coefficient and impulse response function of the tissue.

The results for the heart and fatty tissue are given in Fig. 6. The fatty tissue has a much lower refractive index than the heart tissue, and it is below the refractive index of quartz across the frequency range measured, where as the refractive index of the heart tissue is above the refractive index of quartz for most of the frequency range. From basic optics, when light enters a medium of higher refractive index there is an 180° phase change; correspondingly, when light enters a medium of lower refractive index there is no phase change. Terahertz light is no exception and that is why the main feature of the impulse response function of the heart tissue has opposite phase (i.e. a minimum) to the impulse response function of the fatty tissue.

Similar measurements were made for the other organs. Statistically significant differences were observed for all combinations of the tissue types below 1.0 THz in the calculated absorption coefficient. Above this frequency, the leg muscle and pancreas results were not significantly different, nor were the heart and pancreas data. Once again, the fat data displayed marked differences when compared to the other lean tissues, suggesting that water content is a key contrast agent at terahertz frequencies as fatty tissue contains less water than the lean tissue.

Understanding the origin of contrast has been a key goal of research in the field of medical spectroscopy. Water has been long thought to be a key component of this contrast mechanism. One of the present authors implemented a finite-difference-time-domain (FDTD) model incorporating a double Debye model in order to simulate the dielectric function of the material [44]. This model is often used to describe the dielectric properties of water, as it splits up the relaxation processes into a fast and slow polarization decay rates. Pickwell and coworkers demonstrated that the double Debye model could be successfully applied to *in vivo* skin samples. This suggested a similar dielectric environment to that of pure water. These models were successfully extended in a later study to account for a two layer system (the stratum corneum and epidermis) that could more closely simulate the response of healthy skin [45].

Next, Pickwell and coworkers carried out the first study comparing healthy and diseased skin tissues as measured with terahertz radiation using the FDTD model [46]. A series of basal cell carcinoma (BCC) tissues from volunteers were measured using transmission THz-TDS, along with corresponding samples of their healthy skin *ex vivo*. Both the refractive index and absorption coefficient for the BCC was found to be higher than that obtained for the healthy tissue across the frequency range investigated (0.15–2 THz), resulting in higher values for the double Debye parameters for the BCC tissue type. Comparison of the *in vivo* terahertz data of healthy and BCC tissues from a previous publication [47] showed that the differences observed *ex vivo* were still present *in vivo*, with the refractive index and absorption coefficient being higher for BCC tissue than normal tissue, and in fact closer to the parameters for water. Similar results were presented in the work of Wallace and coworkers and the authors highlighted that whilst water content appeared to account for a large amount of the

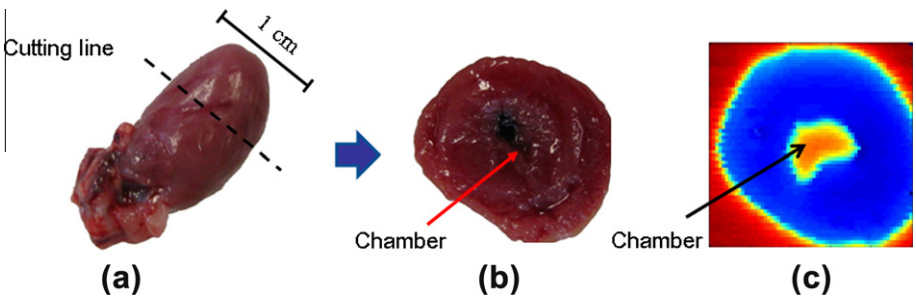

Fig. 5. (a) Photograph of the rat heart tissue used in Ref. [42] highlighting the slice line (b) optical image of the cross-section of the rat heart highlighting the position of the chamber and (c) terahertz image of the same cross-section where the air void due to the chamber can be clearly delineated.

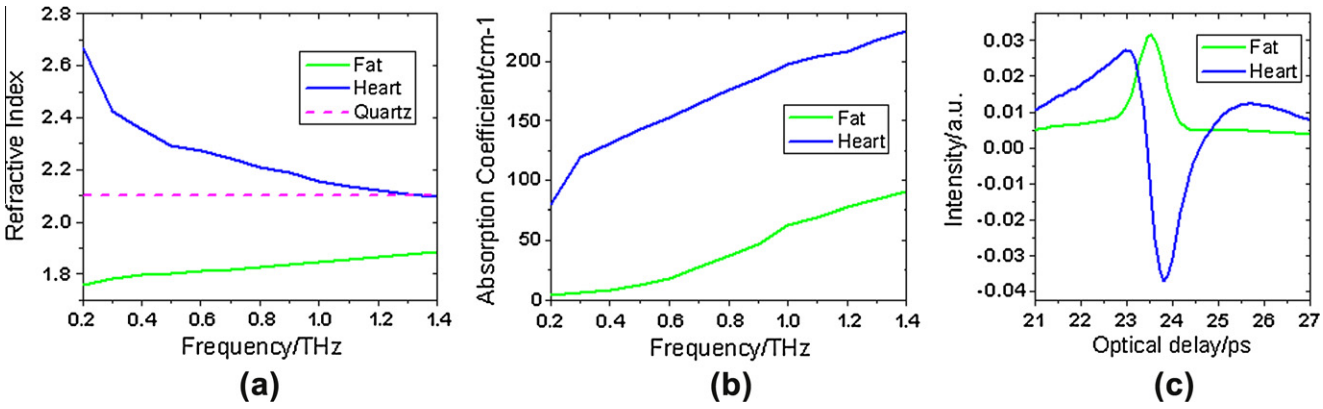

Fig. 6. (a) Refractive index, (b) absorption coefficient and (c) the time-domain response of the fat and heart tissue from the rat samples measured in Ref. [42]. The pink dashed line in (a) highlights the refractive index of quartz.

change in the terahertz results between healthy and diseased tissues, other sources of contrast should be considered [48]. These included structural changes such as increased cell density, and chemical changes such as the relative changes in the concentrations of proteins and lipids.

More recent studies of THz-TDS and cancer diagnosis have diversified from the skin to include other forms of disease affecting the breast and liver. Diagnosis of breast cancer has been a topic of a number of studies [49,50] with the eventual aim to present THz-TDS as an intra-operative tool to compliment histopathology and decrease the need for secondary surgery due to incomplete removal of the cancerous tissue. Fitzgerald and coworkers presented the first studies of excised fresh tumours imaged using THz-TDS [49]. Using a reflection modality, they prepared *x*–*y* sample maps of the sample and observed a clear image contrast between normal and apparently cancerous tissue when plotting parametric images of the minimum of the terahertz impulse function (E_{min}) and the ratio of the minimum to the maximum of the terahertz impulse function (i.e. E_{min}/E_{max}). These parametric images were compared with standard histopathology and the two techniques were found to agree fairly well. The terahertz impulse functions for the tissues are different because the fundamental optical properties of the tissues are different. Fig. 7 shows the refractive index and absorption coefficient of *ex vivo* cancerous tissue (tumour), normal tissue (fibre) and the fatty adipose tissue (adipose). These data were taken from 12 mastectomy patients. Ashworth and coworkers further investigated the spectroscopic signatures of these different tissue types found in a typical breast tumour sample using a transmission geometry [50]. Statistically significant differences in both the absorption coefficient and refractive index between the three tissue types were observed, especially in the refractive index measurements. In particular, there appeared to be a difference maximum observed at approximately 0.32 THz. Simulations of the expected measured reflection pulses from these tissues suggested statistically significant differences consistent with those observed in Ref. [49]. Such results suggest that THz-TDS has a promising future in aiding with the diagnosis and operative success of tumour excision.

Most recently, liver cirrhosis has been investigated using THz-TDS by the present group which has revealed new understanding into the mechanism of contrast between healthy and diseased tissues. Sy and coworkers performed a study of a number of cirrhotic and healthy rat liver samples using THz-TDS and compared the results for both the freshly excised samples and the same samples after formalin fixing to remove the water [51]. As illustrated in Fig. 8, the absorption coefficient of the cirrhotic liver samples was found to be significantly higher than the healthy sample before and after formalin fixing. To estimate the contribution of water to the difference in absorption coefficient, a difference plot is given in Fig. 9. Since the formalin fixing should have removed the contrast due to differences in water content the remaining difference is attributed to structural changes in the cirrhotic tissue when compared to the healthy tissue, as confirmed by microscopic analysis of the samples.

3.2. Enhancing contrast

To date, the research carried out into using terahertz radiation to probe the state of medically relevant tissues has shown that this frequency region has some specificity to disease. A fundamental understanding of this difference still eludes researchers, and the previous section has highlighted some of the recent work attempting to answer this problem. However, a second important area of research is looking into how to enhance signal contrast between different tissue types in order to facilitate diagnosis and further the understanding of the physical and chemical differences between different tissues, whether they are healthy or diseased, or simply different tissue types. For the purposes of this review, contrast enhancement broadly falls into two categories: physical enhancement such as freezing, formalin fixing or using a contrast agent, and signal manipulation – using signal processing tools to highlight different terahertz signals due to physical differences between two samples.

Freezing tissue to suppress the intermolecular interactions of liquid water is one technique that has been researched in recent years. Png and coworkers from the group of Abbott have monitored the hydration dependence of the terahertz signal from fresh rat tissue samples and investigated the feasibility of using lyophilisation (freeze drying) to standardize tissue freshness and enhance contrast mechanisms not relating to water content [52,53]. Fresh rat liver samples cut to 1 mm thickness were too attenuating for meaningful terahertz spectra to be recorded, due to the high absorption from the contained water [52]. However, after lyophilisation, the terahertz transmission data was above the noise floor and it was possible to distinguish between many different types of tissue, despite the absence of water, suggesting that there are mechanisms beyond water absorption that give rise to tissue specificity in terahertz measurements. Png and coworkers have also reported initial results regarding the THz-TDS transmission spectra of healthy and Alzheimer's disease brain tissue [53]. Whilst results were preliminary, there appeared to be some small differences between samples determined to be diseased through histopathology, and those that were not. Additionally, it was not reported whether lyophilisation of the brain tissue improved image contrast; it would be interesting to compare the results of these transmission experiments with similar THz-TDS reflection measurements, where signal attenuation is not such a

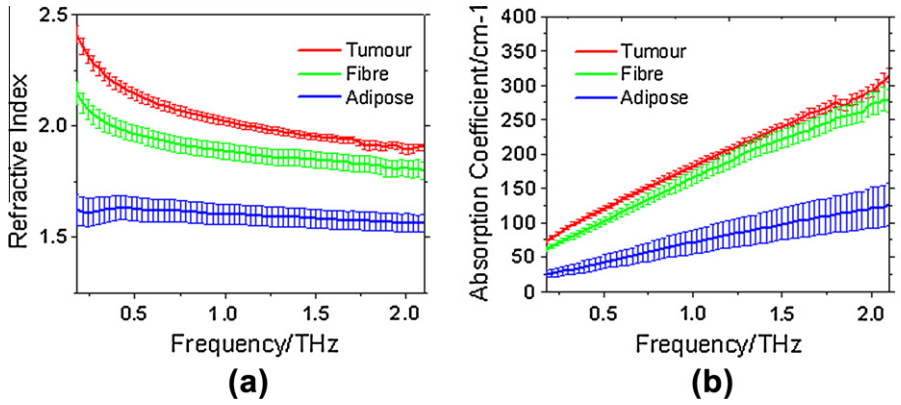

Fig. 7. Average (a) refractive indices and (b) absorption coefficients for tumour, fibrous and adipose tissue taken from a sample of 12 mastectomy patients from 0.2 to 2.1 THz.

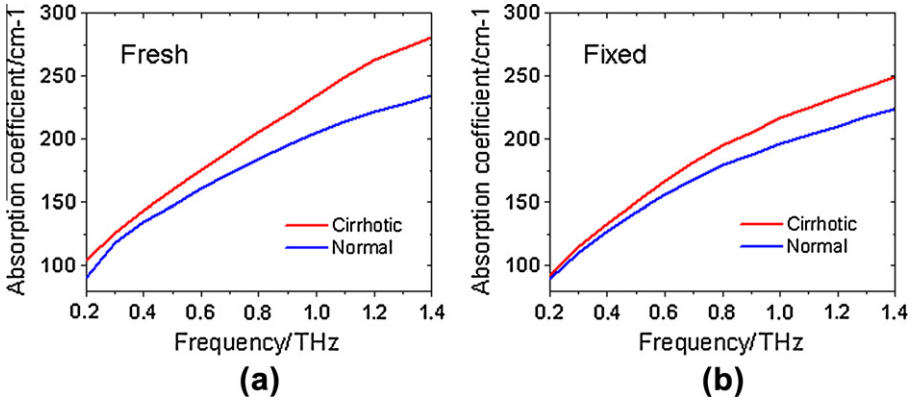

Fig. 8. Absorption coefficients for cirrhotic (red) and normal (blue) rat liver either (a) freshly excised or (b) after formalin fixing. (For interpretation of the references to colour in this figure legend, the reader is referred to the web version of this article.)

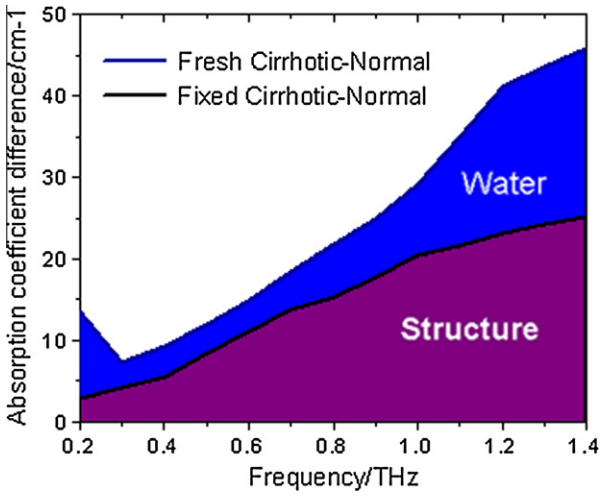

Fig. 9. Difference spectrum comparing cirrhotic to normal tissue. The regions correspond to the contribution of the difference to water and structure respectively, as calculated from the fresh and fixed samples in Fig. 8.

problem for surface measurements. Finally, frozen tissue measurements of porcine tissue have been carried out by Hoshina and coworkers [54]. Here they reported the ability to distinguish between adipose and striated porcine tissue using a transmission THz-TDS system through a thickness of 1.7 mm after freezing. The results suggest that freezing, and in particular freeze drying may be a useful technique for enhancing sensitivity to contrast mechanisms other than water content at terahertz frequencies.

Freeze drying is not the only way to remove the effect of bulk water from medical tissues measured using terahertz. An alternative method used in various *in vitro* studies of medical samples using terahertz radiation is formalin fixing, due primarily as it is a common step in the preparation of samples for histopathology. Sun and coworkers recently documented the changes arising from formalin fixing in the terahertz signatures of porcine adipose and skeletal muscle tissues [55]. The researchers observed that the refractive index and absorption coefficient decreased upon formalin fixing until reaching a plateau after 72 hours of fixing. The changes in the refractive index of the muscle are plotted in Fig. 10a. The fresh tissue has a refractive index that is higher than that of quartz throughout the frequency range, but the fixing process reduces the refractive index so much that after 48 h of fixing, the refractive index of the muscle is lower than that of quartz for frequencies above 0.5 THz. This causes a small peak to appear before the main trough in the impulse response function, as illustrated in Fig. 10b. The peak becomes larger as the refractive index decreases. The refractive index and absorption coefficient of the fatty tissue did not decrease as much as the muscle tissue during the fixing process. However, even after fixing it was possible to distinguish between the skeletal muscle and tissue samples, implying that the different water contents was not the sole contrast mechanism.

Oh and coworkers have made some preliminary studies into using gold nanoparticles as a contrast enhancing agent in THz-TDS spectroscopy [56]. The idea is to insert gold nanoparticles into a tissue (or preferentially bind them to particular tissue types)

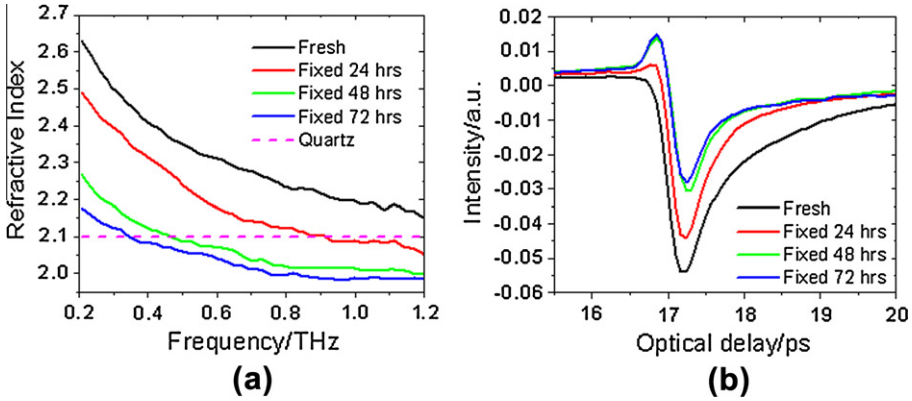

Fig. 10. (a) Refractive index and (b) time-domain results for a series of tissues either fresh or formalin fixed for between 24 and 72 h.

and then to irradiate with IR radiation. The tissue with the gold nanoparticles will be heated up to a greater extent than those without the contrast agent, altering the dielectric properties of the water [57]. The researchers have demonstrated increased reflection from tissues with the gold nanoparticles inserted.

These techniques to increase, or alter in some way, the contrast mechanism have shown some promise, however a key positive factor for using terahertz radiation in a medical situation is its non-invasive, non-ionising nature and so for *in vivo* applications it would be preferable to achieve contrast enhancement through signal processing methods. One technique in particular has received some attention: wavelet based de-noising methods. The wavelet transform allows analysis of a signal in terms of time-localised, oscillating functions. As Mittleman highlighted, the terahertz pulse is localised in time, and indeed closely resembles certain wavelet sets, so it would seem to be an ideal system with which to employ wavelet-based analysis [58]. Wavelet methods applied to THz-TDS in medical imaging have mainly been interested in de-noising the raw data in order to extract as much information as possible from the terahertz pulse. Wavelet de-noising works by first decomposing the signal into the wavelet basis sets before reconstructing the signal using a subset of those sets. Ferguson and Abbott evaluated wavelet de-noising using a number of standard wavelet basis functions on porcine muscle and fatty tissue and found in general an improvement in the signal-to-noise ratio (SNR) [59]. Their work noted that the choice of wavelet function and basis was an important consideration in the success of the de-noising. Validation of any de-noising algorithms is a key consideration when proposing such methods: a well-validated method increases the confidence that the findings enhanced by these techniques are "real" signals and not a result of the method itself. Handley and co-workers addressed these issues by comparing the absorption coefficient and refractive index of a nylon wedge test sample calculated before and after wavelet de-noising [60]. They found that reconstruction of the signal using 20% of the basis sets significantly reduced the noise of the signal and "cleaned up" the time-domain representation, but without altering the absorption coefficient and refractive index. Finally, Chen and coworkers took this technique further by employing wavelet de-noising (frequency-wavelet domain deconvolution, abbreviated FWDD) to improve the signal quality of a terahertz pulse and extract information on the thickness of the stratum corneum from palm data [61]. As with the work of Handley, the wavelet technique was validated by comparing the absorption coefficient and refractive index data extracted from a known test sample, in this case propanol. As depicted in Fig. 11 the de-noised terahertz pulse from the palm displayed a second trough which was not able to be resolved using frequency domain deconvolution with a band pass filter. The second trough was attributed to the stratum corneum-epidermis interface, and agreed with earlier work on terahertz imaging of palm data that had been undertaken on a system with higher SNR [62]. However, it is important to bear in mind that key to any application of wavelet techniques is an understanding of the technique being employed to ensure that artefacts are not introduced in the signal processing stage.

3.3. Other medical applications

Whilst the bulk of work in medical terahertz measurements has focused on soft tissues such as skin, fat and muscle tissues, there have been a limited number of studies into using terahertz radiation to study the hard tissues of the body, such as the teeth and bone. A study of bone density using THz-TDS was undertaken by Stringer and coworkers [63]. They found that there was little use in employing THz-TDS to study bone density, as the only useful correlation appeared to be between terahertz transmission and bone density. There appeared to be little relationship between the refractive index and the Young's modulus, and so the mechanical properties of the bone cannot be elucidated from a terahertz study. In addition, the authors caution that hydration of the bone appears to be an important variable which is not easily controlled in an *in vivo* study of this material.

Crawley and coworkers presented the first studies of THz-TDS and its potential application to monitoring dental health [64,65]. They were able to show that by using the time-of-flight property of reflection-mode THz-TDS it was possible to measure the position of the enamel-dentine boundary to within an accuracy of 10 μm [64]. In a parallel study, using both transmission and reflection imaging it was possible to detect dental caries, the precursor to tooth

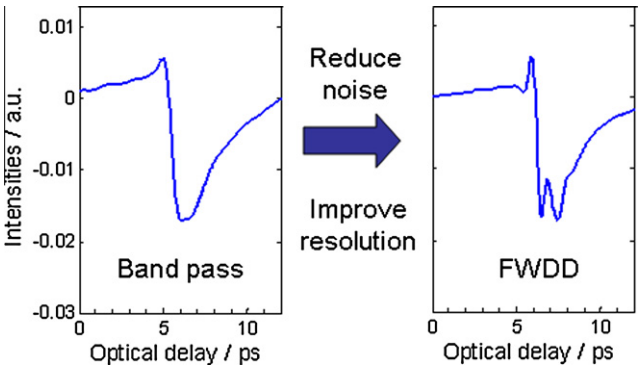

Fig. 11. Terahertz time-domain waveforms of palm data after treatment either with a band pass filter (left) or using the FWDD algorithm (right).

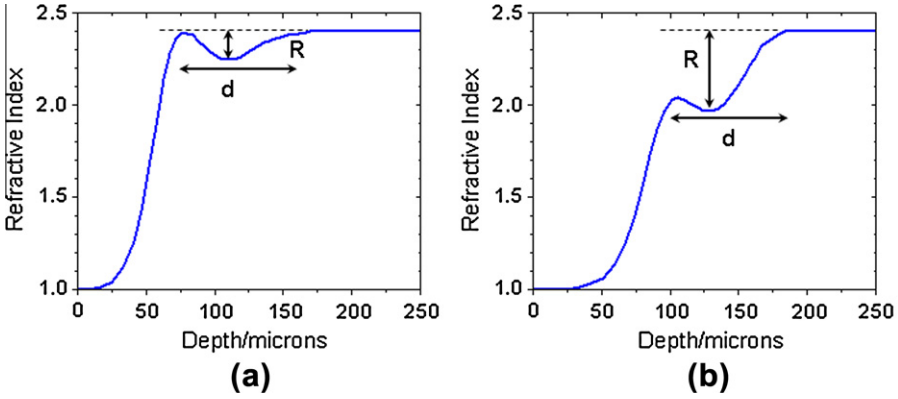

Fig. 12. Terahertz refractive index plots as a function of penetration depth for two teeth demineralisation regions (legions). *R* and *d* are measurements of the demineralisation and lesion thickness respectively.

decay, from the change in terahertz properties when compared to healthy enamel and dentine [65]. Transmission images were able to distinguish between areas of hypomineralisation and caries, and the caries were visible in both transmission and reflection images. The researchers noted that the absorption coefficient difference between normal and carious enamel was approximately 35% in the terahertz region, compared to only 2% in conventional radiographs, suggesting that terahertz imaging techniques will generate higher contrast images, thereby increasing sensitivity. Pickwell and coworkers investigated enamel demineralization *in vitro* using reflection-imaging THz-TDS [66]. It was found that using THz-TDS it was possible to resolve the demineralization region. As shown in Fig. 12, values for R and d, the dimineralisation factor and lesion thickness respectively, could be estimated from the terahertz refractive index profile. This was possible as the refractive index profile calculated from THz-TDS was found to be similar to the mineral content profile calculated from transmission microradiography, suggesting that the refractive index is directly related to the mineral content. These results imply that if suitable probes are designed, THz-TDS may be a useful tool for *in vivo* studies of dental health.

4. Summary

The ability to probe the low-energy, long-wavelength intermolecular interactions of biomolecules using terahertz is a promising proving ground for terahertz technology. However, a key difficulty in interpreting the spectra is the lack of observable, distinct vibrational modes. The issue of overlapping states and the population of many energy levels at terahertz energies makes interpretation of these spectra challenging. In addition, the naturally aqueous environments of biomolecules presents further challenges to THz-TDS, due to the high absorption. Recently, researchers are starting to understand how water interacts with these biomolecules and have begun to be able to interpret the observed results in this frequency range. An understanding of the interaction of biomolecules with water is also advantageous for terahertz medical imaging. This is because a clearer understanding of the interaction of terahertz radiation with biomolecular systems will lead to greater clarity regarding the contrast mechanisms in terahertz images of biomedical samples. A key contrast indicator has long been thought to be water content, but as some recent research has shown there are also significant contributions from structural changes in tissues, and it would not be surprising if the biomolecular changes in these tissues also have an effect.

Within both of these fields, there are still many questions to answer. In the field of biomolecules, a more precise understanding of the interaction of water with these molecules would be invaluable, as well as gleaning a greater insight into the changes to the energy landscape that happens when these large molecules undergo conformational changes. This requires further work into the computational modelling of these molecules, and validation with experiment. In the field of medical spectroscopy, a comprehensive investigation of the contrast mechanisms in tissue, be it water content, structural or biomolecule content based will represent an important step towards a fundamental understanding of the various biological and structural changes that occur between healthy and diseased tissue. With this knowledge, new imaging protocols may be designed to fully realize the potential of terahertz radiation in this field.

Acknowledgments

We gratefully acknowledge partial financial support for this work from the Research Grants Council of the Hong Kong Government (Project Number 419609) and the Shun Hing Institute of Advanced Engineering, Hong Kong.

References

[1] R.A. Cheville, D. Grischkowsky, Opt. Lett. 20 (1995) 1646–1648.
[2] J.A. Zeitler, P.F. Taday, K.C. Gordon, M. Pepper, T. Rades, Chem. Phys. Chem. 8 (2007) 1924–1927.
[3] T.I. Jeon, D. Grischkowsky, Appl. Phys. Lett. 72 (1998) 3032.
[4] J.E. Pedersen, V.G. Lyssenko, J.M. Hvam, P.U. Jepsen, S.R. Keiding, C.B. Sørensen, P.E. Lindelof, Appl. Phys. Lett. 62 (1993) 1265–1267.
[5] O. Esenturk, J.S. Melinger, E.J. Heilweil, J. Appl. Phys. 103 (2008) 23102.
[6] T.-I. Jeon, K.-J. Kim, C. Kang, S.-J. Oh, J.-H. Son, K.H. An, D.J. Bae, Y.H. Lee, Appl. Phys. Lett. 80 (2002) 3403–3405.
[7] E.P.J. Parrott, J.A. Zeitler, J. McGregor, S.-P. Oei, H.E. Unalan, W.I. Milne, J.-P. Tessonnier, D.S. Su, R. Schlögl, L.F. Gladden, Adv. Mater. 21 (2009) 3953–3957.
[8] D.H. Auston, Appl. Phys. Lett. 26 (1975) 101.
[9] C. Fattinger, D. Grischkowsky, Appl. Phys. Lett. 54 (1989) 490–492.
[10] Q. Wu, X.-C. Zhang, Appl. Phys. Lett. 67 (1995) 3523.
[11] H. Harde, S.R. Keiding, D. Grischkowsky, J. Opt. Soc. Am. B 8 (1991) 1642–1651.
[12] P.U. Jepsen, D.G. Cooke, M. Koch, Laser Photon. Rev. 43 (2010).
[13] J.A. Zeitler, P.F. Taday, D.A. Newnham, M. Pepper, K.C. Gordon, T. Rades, J. Pharm. Pharmacol. 59 (2007) 209–223.
[14] E.P.J. Parrott, J.A. Zeitler, T. Friscić, M. Pepper, W. Jones, G.M. Day, L.F. Gladden, Cryst. Growth Des. 9 (2009) 1452–1460.
[15] B. Brooks, M. Karplus, Proc. Nat. Acad. Sci. USA 82 (1985) 4995–4999.
[16] Y. Seno, N. Go, J. Mol. Biol. 216 (1990) 111–126.
[17] T. Globus, D. Woolard, T.W. Crowe, T. Khromova, B. Gelmont, J. Hesler, J. Phys. D: Appl. Phys. 39 (2006) 3405–3413.
[18] A. Markelz, A. Roitberg, E. Heilweil, Chem. Phys. Lett. 320 (2000) 42–48.
[19] M. Kutteruf, C.M. Brown, L.K. Iwaki, M.B. Campbell, T.M. Korter, E.J. Heilweil, Chem. Phys. Lett. 375 (2003) 337–343.
[20] T. Korter, R. Balu, M. Campbell, M. Beard, S. Gregurick, E. Heilweil, Chem. Phys. Lett. 418 (2006) 65–70.
[21] R. Rungsawang, Y. Ueno, I. Tomita, K. Ajito, J. Phys. Chem. B 110 (2006) 21259–21263.
[22] N. Kikuchi, T. Tanno, M. Watanabe, T. Kurabayashi, Anal. Sci. 25 (2009) 457–459.
[23] D.F. Plusquellic, K. Siegrist, E.J. Heilweil, O. Esenturk, ChemPhysChem. 8 (2007) 2412–2431.

[24] K. Yamamoto, K. Tominaga, H. Sasakawa, A. Tamura, H. Murakami, H. Ohtake, N. Sarukura, Biophys. J. 89 (2005) L22–L24.
[25] S.N. Taraskin, S.I. Simdyankin, S.R. Elliott, J.R. Neilson, T. Lo, Phys. Rev. Lett. 97 (2006) 1–4.
[26] E.P.J. Parrott, J.A. Zeitler, L.F. Gladden, S.N. Taraskin, S.R. Elliott, J. Non-Cryst. Solids 355 (2009) 1824–1827.
[27] E.P.J. Parrott, J.A. Zeitler, G. Simon, B. Hehlen, L.F. Gladden, S.N. Taraskin, S.R. Elliott, Phys. Rev. B 82 (2010) 140203.
[28] O. Kambara, A. Tamura, T. Uchino, K. Yamamoto, K. Tominaga, Biopolymers 93 (2010) 735–739.
[29] A. Wittlin, L. Genzel, F. Kremer, S. Häseler, A. Poglitsch, A. Rupprecht, Phys. Rev. A 34 (1986) 493–500.
[30] M. Brucherseifer, M. Nagel, P. Haring Bolivar, H. Kurz, A. Bosserhoff, R. Büttner, Appl. Phys. Lett. 77 (2000) 4049.
[31] B.M. Fischer, M. Walther, P.U. Jepsen, Phys. Med. Biol. 47 (2002) 3807–3814.
[32] M. Bykhovskaia, B. Gelmont, T. Globus, D.L. Woolard, A.C. Samuels, T.H. Duong, K. Zakrzewska, Theor. Chem. Acc. 106 (2001) 22–27.
[33] T.R. Globus, D.L. Woolard, A.C. Samuels, B.L. Gelmont, J. Hesler, T.W. Crowe, M. Bykhovskaia, J. Appl. Phys. 91 (2002) 6105.
[34] R. Parthasarathy, T. Globus, T. Khromova, N. Swami, D. Woolard, Appl. Phys. Lett. 87 (2005) 113901.
[35] S.E. Whitmire, D. Wolpert, A.G. Markelz, J.R. Hillebrecht, J. Galan, R.R. Birge, Biophys. J. 85 (2003) 1269–1277.
[36] R. Balu, H. Zhang, E. Zukowski, J.-Y. Chen, A.G. Markelz, S.K. Gregurick, Biophys. J. 94 (2008) 3217–3226.
[37] J. Knab, J.-Y. Chen, A. Markelz, Biophys. J. 90 (2006) 2576–2581.
[38] J.R. Knab, J.-Y. Chen, Y. He, A.G. Markelz, in: Proc. IEEE, vol. 95, 2007, pp. 1605–1610.
[39] J.-Y. Chen, J.R. Knab, S. Ye, Y. He, A.G. Markelz, Appl. Phys. Lett. 90 (2007) 243901.
[40] Y. Sun, Y.-T. Zhang, E. Pickwell-Macpherson, Biophys. J. 100 (2011) 225–231.
[41] A. Fitzgerald, E. Berry, N. Zinov'ev, S. Homer-Vanniasinkam, R. Miles, J. Chamberlain, M. Smith, J. Biol. Phys. 29 (2003) 123–128.
[42] S.Y. Huang, Y.X.J. Wang, D.K.W. Yeung, A.T. Ahuja, Y.-T. Zhang, E. Pickwell-Macpherson, Phys. Med. Biol. 54 (2009) 149–160.
[43] M. He, A. Azad, S. Ye, W. Zhang, Opt. Commun. 259 (2006) 389–392.
[44] E. Pickwell, B.E. Cole, A.J. Fitzgerald, V.P. Wallace, M. Pepper, Appl. Phys. Lett. 84 (2004) 2190.
[45] E. Pickwell, B.E. Cole, A.J. Fitzgerald, M. Pepper, V.P. Wallace, Phys. Med. Biol. 49 (2004) 1595–1607.
[46] E. Pickwell, A.J. Fitzgerald, B.E. Cole, P.F. Taday, R.J. Pye, T. Ha, M. Pepper, V.P. Wallace, J. Biomed. Opt. 10 (2005) 64021.
[47] V.P. Wallace, A.J. Fitzgerald, S. Shankar, N. Flanagan, R. Pye, J. Cluff, D.D. Arnone, Brit. J. Dermatol. 151 (2004) 424–432.
[48] V.P. Wallace, A.J. Fitzgerald, E. Pickwell, R.J. Pye, P.F. Taday, N. Flanagan, T. Ha, Appl. Spectrosc. 60 (2006) 1127–1133.
[49] A.J. Fitzgerald, V.P. Wallace, M. Jimenez-Linan, L. Bobrow, R.J. Pye, A.D. Purushotham, D.D. Arnone, Radiology 239 (2006) 533–540.
[50] P.C. Ashworth, E. Pickwell-MacPherson, E. Provenzano, S.E. Pinder, A.D. Purushotham, M. Pepper, V.P. Wallace, Opt. Express 17 (2009) 12444–12454.
[51] S. Sy, S. Huang, Y.-X.J. Wang, J. Yu, A.T. Ahuja, Y.-T. Zhang, E. Pickwell-Macpherson, Phys. Med. Biol. 55 (2010) 7587–7596.
[52] G.M. Png, J.W. Choi, B.W.-H. Ng, S.P. Mickan, D. Abbott, X.-C. Zhang, Phys. Med. Biol. 53 (2008) 3501–3517.
[53] G.M. Png, R. Flook, B.W.-H. Ng, D. Abbott, Electron. Lett. 45 (2009) 343–345.
[54] H. Hoshina, A. Hayashi, N. Miyoshi, F. Miyamaru, C. Otani, Appl. Phys. Lett. 94 (2009) 123901.
[55] Y. Sun, B.M. Fischer, E. Pickwell-MacPherson, J. Biomed. Opt. 14 (2009) 064017-7.
[56] S.J. Oh, J. Kang, I. Maeng, J.-S. Suh, Y.-M. Huh, S. Haam, J.-H. Son, Opt. Express 17 (2009) 3469–3475.
[57] C. Rønne, L. Thrane, P.-O. Åstrand, A. Wallqvist, K.V. Mikkelsen, S.R. Keiding, J. Chem. Phys. 107 (1997) 5319.
[58] D.M. Mittleman, R.H. Jacobsen, R. Neelamani, R.G. Baraniuk, M.C. Nuss, Appl. Phys. B 67 (1998) 379–390.
[59] B. Ferguson, D. Abbott, Microelectron. J. 32 (2001) 943–953.
[60] J. Handley, A. Fitzgerald, E. Berry, R. Boyle, Phys. Med. Biol. 47 (2002) 3885–3892.
[61] Y. Chen, S. Huang, E. Pickwell-MacPherson, Opt. Express 18 (2010) 1177–1190.
[62] B.E. Cole, R.M. Woodward, D.A. Crawley, V.P. Wallace, D.D. Arnone, M. Pepper, Proc. Soc. Photo Opt. Instrum. Eng. 4276 (2001) 1–10.
[63] M.R. Stringer, D.N. Lund, A.P. Foulds, A. Uddin, E. Berry, R.E. Miles, A.G. Davies, Phys. Med. Biol. 3211 (2005) 3211–3219.
[64] D. Crawley, C. Longbottom, V.P. Wallace, B. Cole, D. Arnone, M. Pepper, J. Biomed. Opt. 8 (2003) 303.
[65] D.A. Crawley, C. Longbottom, B.E. Cole, C.M. Ciesla, D. Arnone, V.P. Wallace, M. Pepper, Caries. Res. 37 (2003) 352–359.
[66] E. Pickwell, V.P. Wallace, B.E. Cole, S. Ali, C. Longbottom, R.J.M. Lynch, M. Pepper, Caries Res. 41 (2007) 49–55.